Revised paper submitted to HAZMAT (September 20, 2021)

Evaluation of thallium isotopic fractionation during the metallurgical processing of sulfides: an update

Aleš Vaněk[a,*], Kateřina Vejvodová[a], Martin Mihaljevič[b], Vojtěch Ettler[b], Jakub Trubač[b], Maria Vaňková[b], Leslaw Teper[c], Jerzy Cabala[c], Katarzyna Sutkowska[c], Andreas Voegelin[d], Jörg Göttlicher[e], Ondřej Holubík[a], Petra Vokurková[a], Lenka Pavlů[a], Ivana Galušková[a], Tereza Zádorová[a]

[a] Department of Soil Science and Soil Protection, Faculty of Agrobiology, Food and Natural Resources, Czech University of Life Sciences Prague, Kamýcká 129, 165 00 Praha 6, Czech Republic

[b] Institute of Geochemistry, Mineralogy and Mineral Resources, Faculty of Science, Charles University, Albertov 6, 128 00 Praha 2, Czech Republic

[c] Institute of Earth Sciences, Faculty of Natural Sciences, University of Silesia, Bedzinska 60, 41-200 Sosnowiec, Poland

[d] Eawag, Swiss Federal Institute of Aquatic Science and Technology, Ueberlandstrasse 133, CH-8600 Duebendorf, Switzerland

[e] Institute for Photon Science and Synchrotron Radiation, Karlsruhe Institute of Technology, KIT Campus North, Hermann-von-Helmholtz-Platz 1, D-76344 Eggenstein-Leopoldshafen, Germany

---

* Corresponding author (Tel.: +420 224 382 752, Fax: +420 234 381 836)
E-mail: vaneka@af.czu.cz

Highlights

- Thallium(I) – a major form in sulfide concentrates and metallurgical wastes.
- No redox Tl reactions during sulfide processing, as revealed by XANES.
- Overall small Tl isotopic variability (~1 ε^{205}Tl) in the studied samples.
- Minimum Tl isotopic effects throughout the industrial process.

Graphical abstract

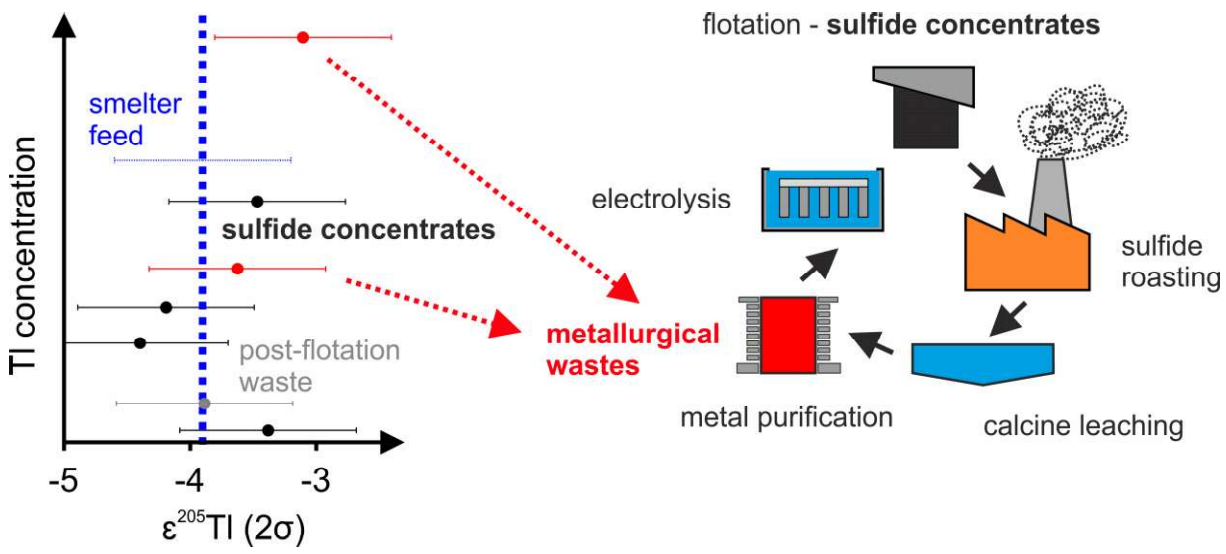

Abstract

In this study, we report combined Tl isotopic and Tl mineralogical and speciation data from a set of Tl-rich sulfide concentrates and technological wastes from hydrometallurgical Zn extraction. We also present the first evaluation of Tl isotopic ratios over a cycle of sulfide processing, from the ore flotation to pyro- and hydrometallurgical stages. The results demonstrate that the prevailing Tl form in all samples is Tl(I), without any preferential incorporation into sulfides or Tl-containing secondary phases, indicating an absence of Tl redox reactions. Although the Tl concentrations varied significantly in the studied samples (~9-280 mg/kg), the overall Tl isotopic variability was small, in the range of -3.1 and -4.4 ±0.7 (2σ) ε^{205}Tl units. By combining present ε^{205}Tl results with the trends first found for a local roasting plant, it is possible to infer minimum Tl isotopic effects throughout the studied industrial process. As a result, the use of Tl isotopic ratios as a source proxy may be complicated or even impossible in areas with naturally high/extreme Tl background contents. On the other hand, areas with two or more isotopically contrasting Tl sources allow for relatively easy tracing, i.e., in compartments which do not suffer from post-depositional isotopic redistributions.

Keywords: Waste; Metallurgy; Isotopic Fractionation; Speciation

1. Introduction

Thallium (Tl) is a toxic trace element (metal) included in the US EPA list of priority toxic pollutants (Kazantzis, 2000). Because of its acute and chronic toxicity for most living organisms (comparable to e.g. Hg or Cd) (John Peter and Viraraghavan, 2005), Tl can be thought as one of the most dangerous elements in the environment. Since metal sulfides tend to accumulate Tl (e.g., FeS_2 and ZnS), their mining, metallurgical processing and co-processing (mine waste recycling) all represent potential pathways of Tl entry into the environment (Kazantzis, 2000; Xiao et al., 2004, 2012; John Peter and Viraraghavan, 2005; Jakubowska et al., 2007; Karbowska et al., 2014; Gomez-Gonzalez et al., 2015; Liu et al., 2016, 2019; Aguilar-Carrillo et al, 2018; Garrido et al., 2020; Wei et al., 2021; Ning et al., 2021). Thallium may occur in K-silicates (K-feldspars, micas) or may specifically be adsorbed by micaceous clay minerals (mainly illite), mostly reflecting ion Tl(I)-K(I) exchange reactions. Furthermore, Tl-containing sulfide and oxide associations, including Tl(III) forms, are reported as important Tl pools or sinks in the environment (Fe-Zn sulfide deposits, Fe-Mn crusts/nodules, etc.) (Tremel et al., 1997; Jović, 1998; Jacobson et al., 2005a, 2005b; Vaněk et al., 2011, 2013; Voegelin et al., 2015; Nielsen et al., 2017). It should be noted that Tl has two stable isotopes (^{205}Tl and ^{203}Tl) with average abundances of ~70% and ~30%, respectively. Despite recent achievements in Tl isotope geochemistry in Earth and environmental sciences (Rehkämper et al., 2002, 2004; Peacock and Moon, 2012; Nielsen et al., 2013, 2017; Prytulak et al., 2013, 2017; Vaněk et al., 2016, 2019, 2020; Owens et al., 2017; Grösslová et al., 2018; Howarth et al., 2018; Rader et al., 2018, 2019; Ostrander et al., 2019, 2020; Vejvodová et al., 2020, etc.), still very little is known about the behavior of stable Tl isotopes during industrial activities. For example, we do not know to what degree Tl isotope fractionation can take place during metallurgical sulfide processing, involving all the stages such as ore flotation, pyrometallurgy as well as hydrometallurgy. The only available Tl isotopic data and related

effects are known for different waste materials from specific high-temperature operations (ore roasting, coal burning) – various fly ashes/dusts, slags, etc. (Vaněk et al., 2016, 2018; Liu et al., 2020). The major findings can be summarized as follows: (i) partial Tl isotopic fractionation can potentially take place during high-temperature activities, with isotopically lighter Tl present in fly ash relative to remaining slag or bottom ash (enriched in heavy ^{205}Tl isotope); (ii) the volatile Tl fractions present in gas/vapor phases tend to be enriched in light ^{203}Tl isotope, probably due to its higher reaction rate during evaporation (Vaněk et al., 2016, 2018).

However, to be able to assess the behavior/fate of Tl stable isotopes throughout the metallurgical processes, the isotopic signatures of the feed treatment or final/base metal solution refinement(s) are clearly yet to be determined. In this study, we report combined Tl isotopic and Tl mineralogical and speciation data from a set of Tl-rich sulfide concentrates and technological wastes from hydrometallurgical Zn extraction. We attempt to answer the following fundamental questions: (i) How does the hydrometallurgical process influence complex Tl chemistry, i.e., what are major smelter-derived Tl-containing phases? (ii) Do changes in Tl chemistry reflect the changes in Tl isotopic composition in metallurgical wastes? (iii) To what degree can Tl isotopes be redistributed during a complete industrial cycle (pyro- and hydrometallurgy) relative to the primary Tl source (ore)?

The work follows our earlier Tl isotopic research from a roasting/Waelz technology (Vaněk et al., 2018) and it offers new insights into stable Tl isotope signatures in source materials of anthropogenic origin, which can potentially be used to assess industrial Tl inputs in the environment.

2. Experimental

2.1 Ore and processing waste samples

A set of Zn-rich sulfide concentrates and selected processing wastes (sludges) from the hydrometallurgy of Zn were investigated in this work. All studied samples originate from specific (MVT – "the Mississippi Valley"-type) sulfide deposits located in Europe and Asia (Olkusz, Poland; Lisheen, Ireland; Pinargozu, Turkey) and were simultaneously processed in the Boleslaw Zn smelter (southern Poland) in November 2020. Detailed information about the samples, their location within the industrial process (Fig. S1), sample mineralogy and chemistry are given in the Supplementary Material section.

2.2 Mineralogical characterization and Tl speciation

The phase compositions of the studied samples were determined by X-ray diffraction analysis (XRD) (X'Pert Pro diffractometer, PANalytical, the Netherlands) under the following conditions: CuKα radiation at 40 kV (30 mA), 2 theta range of 5-80°, counting time of 150 sec per step (step of 0.02°). The obtained diffraction patterns were processed using X'Pert High Score Plus 3.0 software, in combination with a Crystallography Open Database (COD) (Gražulis et al., 2012). Selected ore/waste samples (1, 4, and 6) were studied using scanning electron microscopy (SEM) and electron probe microanalysis (EPMA). A JEOL JXA-8530F (JEOL, Japan) electron probe microanalyzer with a field emission gun as an electron source and an energy dispersion spectrometer (EDS) (JEOL JED-2300F) was used. This instrument was also used for quantitative microanalysis. The EPMA operating conditions, calibration standards and detection limits are reported in Table S1 (Supplementary Material).

To gain information on Tl speciation, the samples with the highest Tl concentrations (to eliminate Fe, As, Sb etc. interferences, if present) were analyzed by X-ray absorption near

161 edge structure (XANES) spectroscopy (Tl L_{III}-edge, SUL-X beamline) at the Synchrotron
162 Radiation Source, Karlsruhe Institute of Technology (KIT, Germany). These measurements
163 were performed in fluorescence mode at room temperature. The BCR sequential extraction
164 method was applied to the studied samples as well, using the procedure properly described in
165 Vaněk et al. (2010). The reason was to better assess the role of major Tl-host phases in a
166 complex process of Tl uptake (coprecipitation).
167
168 *2.3 Element concentrations*
169 Samples were air-dried (to a constant weight) prior to Tl/element concentration
170 measurement. A sample aliquot of 0.2 g was dissolved in a mixture of concentrated HNO_3/HF
171 (Merck Ultrapure, Germany) (2:1 ratio, ~20 mL, total volume) and then diluted in 2% HNO_3
172 (50 mL). PTFE beakers (60-mL, Savillex, USA) and a ceramic plate (150-200 °C, 48 h) were
173 utilized throughout this step. Concentrations of Tl, Zn, Pb, and Fe in the individual solutions
174 were determined using Q-ICP-MS (Xseries II, Thermo Scientific, Germany) in a triplicate
175 approach. Standard reference material 2711 (Montana Soil, NIST, USA) was used for the QC
176 of quantitative Tl analysis (Table S2, Supplementary Material).
177
178 *2.4 Thallium isolation*
179 A two-step chemical separation of Tl with Bio-Rad AG1-X8 resin in the Cl^- form
180 without utilizing HBr was used (Supplementary Material). The technique is analogical with
181 those used within our previous studies (Vaněk et al., 2016, 2018, 2019, 2020; Grösslová et al.,
182 2018; Vejvodová et al., 2020).
183
184 *2.5 Thallium isotope measurement*

Detailed information about the measurement of Tl isotopic ratios using MC-ICP-MS Neptune plus (Thermo Scientific, Germany), including the analytical conditions similar to those described in e.g., Prytulak et al. (2013, 2017), and the respective QC (Table S3), are shown in the Supplementary Material section.

3. Results and discussion

3.1 Thallium phase associations by XRD and EPMA

The XRD analysis indicated that the phase composition of the studied concentrates is dominated by sphalerite (ZnS) and pyrite (FeS_2) with minor proportion of other sulfides, secondary sulfates (anglesite, $PbSO_4$; plumbojarosite, $PbFe_6(SO_4)_4(OH)_{12}$; susannite, $Pb_4(SO_4)(CO_3)_2(OH)_2$) and gangue phases such as quartz (SiO_2), dolomite ($CaMg(CO_3)_2$) or calcite ($CaCO_3$) (Fig. S2). In contrast, metallurgical sludges are mainly composed of a spinel-family oxide (franklinite, $ZnFe_2O_4$), sphalerite and sulfates such as plumbojarosite, anglesite and gypsum ($CaSO_4 \cdot 2H_2O$) (Fig. S2). The EPMA data indicate that high concentrations of EPMA-detectable Tl are found in all the sulfides: 0.03-0.09 wt.% in sphalerite, 0.04-0.07 wt.% in pyrite and 0.20 wt.% in galena (Table S4). Given the high proportion of sphalerite (Figs. 1 and S2), this phase is the dominant carrier of Tl in the concentrates, in line with measured Zn concentrations (Table 1). Thallium was also detected in mixtures of secondary Pb phases, where it is probably mainly bound in plumbojarosite, with Tl concentrations in the range 0.06-0.20 wt.% (Table S5). Interestingly, high Tl amounts were also found in franklinite (0.12-0.28 wt.% Tl) and in gypsum (0.30 wt.% Tl) in the Larox sludge sample (Table S6). We assume that this can be a result of Tl coprecipitation with secondary metallurgical phases as a function of Tl concentration in the reaction media, pH, temperature, etc. However, passive Tl sorption can also be promoted by Tl(I) retention in exchangeable K-exchanged positions/layers, for instance, in oxide or sulfate precipitates (Vaněk et al., 2010).

3.2 Thallium speciation by XANES spectroscopy

The Tl L_{III}-edge XANES spectra of selected ore and metallurgical samples (1, 2, 6 and 7) are compared to reference spectra in Fig. 2. In general, the quality of the sample spectra is not ideal because of spectral interferences and fluorescence attenuation caused by the very

high levels of Zn, Pb and As in the samples. Nevertheless, the spectra most closely resemble to the spectra of Tl(I)-aqueous or Tl(I)-sulfide (lorandite), indicating that most Tl is monovalent Tl(I). Due to the limited quality of the sample spectra, the lack of reference spectra for other potential Tl(I) phases, and limited spectral characteristics, our data do not allow to further constrain the speciation of Tl(I) in metallurgical samples. Only for the Larox sludge, do the spectral characteristics suggest that a fraction of the Tl(I) may be incorporated in jarosite, as would be consistent with the literature (Dutrizac, 1997). Regarding the absence of clearly detectable levels of Tl(III), this finding is in agreement with the generally low stability of trivalent Tl(III) species, which start to degrade at relatively low temperatures (~150 °C, $TlCl_3$) as they generally have only limited/low thermal stability (Holleman et al., 1995; Phillips and Perry, 1995; Lide, 2009). Moreover, the formation of Tl(III) species could only be favored under highly oxidative conditions, otherwise Tl(I) species tend to dominate (Vaněk et al., 2016).

Although, the reliability of the BCR sequential extraction in the determination of Tl sources is generally not much high (Vaněk et al., 2010), its combination with all the Tl speciation and mineralogical data allowed us to draw the following key conclusions (Table S7). With the exception of samples 6 and 7 (Larox and Dorr sludges), the samples showed a good geochemical stability, as the majority of Zn and Pb, including Tl, was associated with the oxidizable and residual fractions (Table S7). This finding indicates the dominant role of sulfides in the total process of Tl retention, as well as only limited role of sulfide weathering in Tl release. On the other hand, there is clear evidence for the formation of Tl-containing precipitates (oxides, sulfates) in metallurgical wastes with marked Tl solubility within the acid-extractable and reducible fractions. This behavior strengthens the conclusion that Tl can significantly be mobilized during hydrometallurgical Zn extraction, or the metallurgy of sulfides in general.

260

261 *3.3 Thallium concentrations and isotopic variability in sulfide concentrates*

262 Thallium concentrations in the studied concentrates varied substantially, from 8.6
263 mg/kg (sample 2) to 169 mg/kg (sample 1) (Table 1). All samples are identical in their origin,
264 as they originate from the low-T sulfide mineralizations (<200 °C) of the Mississippi Valley
265 type (MVT) (Supplementary Material). Monovalent Tl, as a relatively conservative trace
266 element with a chemistry similar to K, tends to accumulate in "late" hydrothermal fluids from
267 which it can preferentially enter the specific low/medium-T mineral associations, including
268 sulfides (Hetmann et al., 2014).

269 The Tl isotopic variability observed in the concentrate samples, expressed as ε^{205}Tl,
270 ranged from -3.4 to -4.4 (±0.7). The finding suggests quite uniform isotopic compositions.
271 Considering the ε^{205}Tl value of -3.9 in the post-flotation waste (sample 5) derived from the
272 Olkusz ores with ε^{205}Tl values of -4.4 and -4.2 (samples 3 and 4) (Table 1), it can be argued
273 that initial sulfide pre-concentration did not affect the Tl isotopic signature of the flotation
274 product, which is mostly absent of gangue constituents. In other words, the role of gangue
275 mineralization in total Tl isotopic composition of the Olkusz Zn/Pb deposit is probably not
276 important.

277 It should also be highlighted that the identified overall ε^{205}Tl range, including the
278 lowest ε^{205}Tl value in the concentrate from Olkusz (-4.4), is regularly observed in
279 igneous/hydrothermal and even sedimentary rocks or phases (Prytulak et al., 2013, 2017;
280 Nielsen et al., 2017; Howarth et al., 2018). Hettman et al. (2014) on an example of the MVT
281 deposit in Wiesloch (Germany) demonstrate relatively similar ε^{205}Tl values to our ore-like
282 samples, with ε^{205}Tl = -2.7 (±0.5) for sphalerite or -1.4 for galena. In general, the authors
283 report that the main cause for the Tl isotopic variations in sulfides and accompanying trace
284 metal-bearing minerals like sulfosalts is mass-independent fractionation (MIF), with a nuclear

285 volume-dependent effect as the controlling mechanism. It is assumed that the mass-dependent
286 fractionation (MDF), which is typically associated with kinetic processes of heavy metal
287 isotopes, including Tl, seems to be somewhat suppressed during hydrothermal processes
288 (Hettman et al., 2014). The theory is based on the premise that the diffusivity of Tl in the
289 sulfide melt is possibly much faster than preferential (kinetically-driven) reactions of Tl
290 isotopes over the sulfide formation. By combining all the available Tl isotopic MVT data with
291 the ε^{205}Tl values observed in the Earth's mantle and/or bulk continental crust samples with
292 ε^{205}Tl -2.0 (±1) on average (Nielsen et al., 2006a,b, 2017), this could also be evidence for
293 relatively low/limited stable Tl isotope fractionation during the formation of sulfides within
294 the MVT deposits. Therefore, some consistency in Tl isotopic signatures with the primary
295 magmatic Tl source or differentiated crust-derived melt enriched in Tl could be assumed.
296
297 *3.4 Thallium concentrations and isotopic variability in processing wastes*
298 The metallurgical sludges, with up to 283 mg Tl/kg (Table 1), indicate substantial
299 Tl(I) accumulation, though mainly in specific newly formed oxides and gypsum (Table S6),
300 in line with primary Tl source(s) such as sulfide concentrates (Tables 1 and S4).
301 The calculated (weighted) mean ε^{205}Tl value corresponding to the metallurgical feed
302 material used in the Boleslaw Zn smelter (as for November, 2020), which is a mixture of the
303 concentrates 1, 2 and 3(4) in a ratio of ~1/~1/~2, respectively (Supplementary Material),
304 equals -3.9. This value is analogous to that observed for a local post-flotation waste (Table 1).
305 When ε^{205}Tl values in metallurgical sludges (-3.6 and -3.1, ±0.7) are compared with the
306 smelter feed (-3.9, ±0.7), the data are indicative of a negligible Tl isotopic fractionation. This
307 assumption is also consistent with only small variations in ε^{205}Tl (from -4.1 to -3.3, ±0.7) that
308 we have first observed in all local massive ore and various waste materials from a high-
309 temperature roasting/Waelz process (fly ash, slag and granulated waste) in the same

metallurgical plant (Vaněk et al., 2018). Given the limited isotopic variability in the studied samples of only ~1 ε^{205}Tl (Table 1 and Fig. S1), including that regarding the roasting technology (Vaněk et al., 2018), we assume that sulfide ore processing does not result in significant Tl isotopic fractionation(s), i.e., in terms of a complete industrial Tl cycle. Further evidence for a conservative behavior of stable Tl isotopes can be seen from Fig. 3, which shows that all samples apparently fall in a 2σ range of a mean ε^{205}Tl value (-3.7).

Such an isotopic homogeneity is quite surprising, at least in view of a wide range of Tl concentrations (~9-280 mg/kg) (Table 1) or a very large variability in Tl isotopic ratios in different solid wastes from pyrite roasting technology, yielding ~17 ε^{205}Tl units (from -1 to +16), as recently reported by Liu et al. (2020). Therefore, our results are more similar to data by Kersten et al. (2014), who observed even an absence of Tl isotopic fractionation for a high-temperature process, albeit in relation to cement production. The authors revealed an analogy in the isotopic signature in Tl-rich FeS_2, co-combusted waste from FeS_2 roasting (as an additive) and emitted cement kiln dust (CKD), all exhibiting ε^{205}Tl ~0.

Indeed, our earlier isotopic data for fly ash and slag in the Boleslaw Zn smelter point to isotopically lighter Tl in the fly ash, corresponding to 0.8 ε^{205}Tl unit as a difference (Vaněk et al., 2018). The finding was explained by a higher rate of reaction kinetics of the ^{203}Tl isotope during evaporation, followed by the accumulation of ^{205}Tl in the remaining slag phase. From this viewpoint, the concept is synonymous to that proposed by Liu et al. (2020), who, on the basis of a Rayleigh distillation model, demonstrated marked Tl isotopic fractionation factors of $\alpha_{slag\text{-}vapor}$ = 1.0010-1.0025 between the slag and model vapor phase (Liu et al., 2020). We observed similar behavior in various emitted temperature-controlled Tl vapor and condensate samples (ε^{205} between ~-6 and -10), in comparison to the bottom ash (ε^{205} ~0) from industrial coal burning, thus, exhibiting a total variability of 10 ε^{205}Tl units (Vaněk et al., 2016). However, all the solid materials of fly and bottom ashes derived in the

studied coal-fired power plant (Turów, Poland) showed much lower isotopic variability, which accounted for ~2.5 ε^{205}Tl units (Vaněk et al., 2016). At this point, again, it should be noted that we did not observe similar marked isotopic variations in any solid material or critical reaction products throughout the currently studied metallurgical technology. Moreover, all the identified Tl shifts were insignificant, on the basis of 2σ (Fig. 3).

In contrast, for stable Zn isotopes during primary Cu smelting (Krompachy, Slovakia), Bigalke et al. (2010) proved significant isotopic variations, in fly ash (δ^{66}Zn, -0.41‰) and grained slag and solid waste (0.18‰ and 0.25‰, respectively). This is congruent with data detected by Cloquet et al. (2006) for stable Cd isotopes. Comparable results are also reported by Kříbek et al. (2018) for Cu isotopes from the Cu smelter in Tsumeb (Namibia). The authors revealed isotopically lighter Cu in the fly ash (δ^{65}Cu = +0.15‰) relative to the Cu isotopic signature in the smelter charge (δ^{65}Cu = +0.28 and +0.44‰). All this information, in combination, possibly indicates the ability of lighter trace elements (Zn, Cu, Ni, Cd etc.) to be isotopically redistributed more significantly during both high- and low-temperature metallurgical operations or within anthropogenic activities in general (Wiederhold, 2015; Chrastný et al., 2015).

3.5 Potential link between Tl speciation and Tl isotopic data?

A combination of Tl mineralogical and speciation data and Tl isotopic compositions in the studied samples did not reveal any link between Tl forms and Tl isotopic signature. Omitting the fact that the total number of XANES and EPMA analyses was limited, apparently Tl was mainly present as Tl(I) and ZnS was a dominant Tl-host phase in all concentrate samples (Figs. 1 and S1). Thallium was also detected in other minor sulfides (FeS_2, PbS). Nevertheless, the overall distribution of Tl was relatively uniform in different sulfide minerals (≤0.2 wt.%) (Table S4). Similarly, both the secondary Tl-rich minerals

(mainly sulfates) and metallurgical precipitates (spinel oxides) did not indicate any important shifts in Tl concentrations, all exhibiting ≤0.3 wt.% (Tables S5 and S6).

Regarding the absence of any relationship between Tl(I) speciation and the isotopic Tl signature, we assume that the Tl isotopes can be more efficient as qualitative tracers of the genesis of ore deposits. More specifically, Tl isotopic ratios can successfully be used as tracers of specific inter-element or mineral relationships within a specific deposit/mineralization for which, however, an accurate separation of Tl-rich minerals accompanied by selective Tl isotopic analysis is essential (Hettman et al., 2014; Rader et al., 2018)

4. Environmental implications

Contamination of the environment with Tl due to mining/processing of sulfides has widely been reported (Kazantzis, 2000; Xiao et al., 2004, 2012; Jakubowska et al., 2007; Karbowska et al., 2014; Gomez-Gonzalez et al., 2015; Liu et al., 2016, 2019; Aguilar-Carrillo et al, 2018; Garrido et al., 2020; Wei et al., 2021; Ning et al., 2021). Furthermore, it seems that similarly to industrial coal burning, this activity is potentially responsible for up to 1/4 of global anthropogenic Tl inputs (>0.5 Gg Tl/year) (John Peter and Viraraghavan, 2005).

Here, we present the first evaluation of Tl isotopic ratios over a complex cycle of sulfide processing, from the ore flotation to pyro- and hydrometallurgical stages. We found only insignificant Tl isotopic variations (on the basis of 2σ, 0.7 ε^{205}Tl) between initial smelter feed – sulfide concentrates and the waste materials from hydrometallurgical Zn extraction, in spite of relatively large differences in their Tl concentrations. The present data confirmed a very good consistency with the Tl isotopic data that we first obtained solely within roasting technology in the same plant (Vaněk et al., 2018). In combination, the results point to minimum Tl isotopic effects in terms of a total industrial process.

We found that the prevailing Tl form in all concentrates and metallurgical wastes is Tl(I), without any preferential incorporation into sulfides or Tl-containing secondary phases, mainly sulfates and spinel oxides. Therefore, we expect any reactions which alter Tl redox speciation (oxidation) and which could possibly be expected for some stages of hydrometallurgical processing to be absent. These reactions, if present, could lead to marked Tl isotopic effects (Wiederhold, 2015, Nielsen et al., 2017).

In summary, the obtained Tl isotopic data are similar and mimic the signature of the primary Tl source in all the key stages of sulfide processing. As a result, the use of Tl isotopic ratios as a source proxy or for quantifying industrial emissions may be complicated or even impossible in areas with naturally high/extreme Tl background contents. On the other hand,

areas with two or more isotopically contrasting Tl sources allow for relatively easily tracing (Kersten et al., 2014; Vaněk et al., 2016; Grösslová et al., 2018), for instance, in sediments or soils which do not suffer from post-depositional isotopic redistribution effects.

Acknowledgements

This study was funded by the projects of the Czech Science Foundation (GAČR 20-08717S) and the European Regional Development Fund (CZ.02.1.01/0.0/0.0/16_019/0000845). Charles University researchers also received institutional funding from the Center for Geosphere Dynamics (UNCE/SCI/006). Polish authors were financially supported by the University of Silesia (WNP/INoZ/2020-ZB32). Furthermore, we acknowledge the assistance of Petr Drahota (XRD) and Radim Jedlička (SEM/EDS, EPMA), as well as of Chris Ash (UK) (English editing). Finally, all the anonymous reviewers are thanked for their comments and/or suggestions which improved the quality of the original manuscript version.

460 **References**

461

462 J. Aguilar-Carrillo, L. Herrera, E.J. Gutiérrez, I.A. Reyes-Domínguez, Solid-phase
463 distribution and mobility of thallium in mining-metallurgical residues: Environmental hazard
464 implications, Environ. Pollut. 243 (2018) 1833–1845. DOI: 10.1016/j.envpol.2018.10.014

465

466 M. Bigalke, S. Weyer, J. Kobza, W. Wilcke, Stable Cu and Zn isotope ratios astracers of
467 sources and transport of Cu and Zn in contaminated soil, Geochim.Cosmochim. Acta 74
468 (2010) 6801–6813. DOI: 10.1016/j.gca.2010.08.044

469

470 V. Chrastný, E. Čadková, A. Vaněk, L. Teper, J. Cabala, M. Komárek, Cadmium isotope
471 fractionation within the soil profile complicates source identification in relation to Pb–Zn
472 mining and smelting processes, Chem. Geol. 405 (2015) 1–9. DOI:
473 10.1016/j.chemgeo.2015.04.002

474

475 C. Cloquet, J. Carignan, G. Libourel, T. Sterckeman, E. Perdrix, E., Tracing source pollution
476 in soils using cadmiumand lead isotopes, Environ. Sci. Technol. 40 (2006) 2525–2530. DOI:
477 10.1021/es052232+

478

479 J.E. Dutrizac, The behavior of thallium during jarosite precipitation, Metall Mater Trans B
480 volume 28 (1997) 765–776. DOI: 10.1007/s11663-997-0003-9

481

482 F. Garrido, J. Garcia-Guinea, P. Lopez-Arce, A. Voegelin, J. Göttlicher, S. Mangold, G.
483 Almendros, Thallium and co-genetic trace elements in hydrothermal Fe-Mn deposits of
484 Central Spain, Sci. Total Environ. 717 (2020) 137162. DOI: 10.1016/j.scitotenv.2020.137162

M.A. Gomez-Gonzalez, J. Garcia-Guinea, F. Laborda, F. Garrido, Thallium occurrence and partitioning in soils and sediments affected by mining activities in Madrid province (Spain), Sci. Total Environ. 536 (2015) 268–278. DOI: 10.1016/j.scitotenv.2015.07.033

S. Gražulis, A. Daškevič, A. Merkys, D. Chateigner, L. Lutterotti, M. Quirós, N.R. Serebryanaya, P. Moeck, R.T.Downs, A. Le Bail, A., Crystallography Open Database (COD): an open-access collection of crystal structures and platform for world-wide collaboration, Nucleic Acids Res. 40 (2012) D420–D427. DOI: 10.1093/nar/gkr900

Z. Grösslová, A. Vaněk, V. Oborná, M. Mihaljevič, V. Ettler, J. Trubač, P. Drahota, V. Penížek, L. Pavlů, O. Sracek, B. Kříbek, A. Voegelin, J. Göttlicher, O. Drábek, V. Tejnecký, J. Houška, B. Mapani, T. Zádorová, Thallium contamination of desert soil in Namibia: chemical, mineralogical and isotopic insights, Environ. Pollut. 239 (2018) 272–280. DOI: 10.1016/j.envpol.2018.04.006

K. Hettmann, K. Kreissig, M. Rehkämper, T. Wenzel, R. Mertz-Kraus, G. Markl, Thallium geochemistry in the metamorphic Lengenbach sulfide deposit, Switzerland: Thallium-isotope fractionation in a sulfide melt, Am. Miner. 99 (2014) 793–803. DOI: 10.2138/am.2014.459

A.F. Holleman, E. Wiberg, N. Wiberg, Lehrbuch der Anorganischen Chemie; Walter de Gruyter & Co.: Berlin, NY, 1995.

S. Howarth, J. Prytulak, S.H. Little, S.J. Hammond, M. Widdowson, Thallium concentration and thallium isotope composition of lateritic terrains, Geochim. Cosmochim. Acta 239 (2018) 446–462. DOI: 10.1016/j.gca.2018.04.017

A.R. Jacobson, M.B. McBride, P. Baveye, T.S. Steenhuis, Environmental factors determining the trace-level sorption of silver and thallium to soils, Sci. Total Environ. 345 (2005a) 191–205. DOI: 10.1016/j.scitotenv.2004.10.027

A.R. Jacobson, S. Klitzke, M.B. McBride, P. Baveye, T.S. Steenhuis, The desorption of silver and thallium from soils in the presence of a chelating resin with thiol functional groups, Water Air Soil Pollut. 160 (2005b) 41–54. DOI: 10.1007/s11270-005-3860-3

M. Jakubowska, A. Pasieczna, W. Zembrzuski, Z. Swit, Z. Lukaszewski, Thallium in fractions of soil formed on floodplain terraces, Chemosphere 66 (2007) 611–618. DOI: 10.1016/j.chemosphere.2006.07.098

A.L. John Peter, T. Viraraghavan, Thallium: a review of public health and environmental concerns, Environ. Int. 31 (2005) 493–501. DOI: 10.1016/j.envint.2004.09.003

V. Jović, Thallium, in: C.P. Marshall, R.W. Fairbridge (Eds.), Encyclopedia of Geochemistry, Kluwer Academic Publishers, Dordrecht, Germany, 1998, pp. 622–623.

B. Karbowska, W. Zembrzuski, M. Jakubowska, T. Wojtkowiak, A. Pasieczna, Z. Lukaszewski, Translocation and mobility of thallium from zinc–lead ores, J. Geochem. Explor. 143 (2014) 127–135. DOI: 10.1007/s00128-016-1831-6

G. Kazantzis, Thallium in the environment and health effects, Environ. Geochem. Hlth. 22 (2000) 275–280. DOI: 10.1023/A:1006791514080

M. Kersten, T. Xiao, K. Kreissig, A. Brett, B.J. Coles, M. Rehkämper, Tracing anthropogenic thallium in soil using stable isotope compositions, Environ. Sci. Technol. 48 (2014) 9030–9036. DOI: 10.1021/es501968d

B. Kříbek, A. Šípková, M. Mihaljevič, V. Majer, I. Knésl, B. Mapani, V. Penížek, A. Vaněk, O. Sracek, Variability of the copper isotopic composition in soil and grass affected by mining and smelting in Tsumeb, Namibia, Chem. Geol. 493 (2018) 121–135. DOI: 10.1016/j.chemgeo.2018.05.035

D.R. Lide, Ed., CRC Handbook of Chemistry and Physics, 90th, ed.; CRC Press (Taylor and Francis Group): Boca Raton, FL, 2009.

J. Liu, J. Wang, Y. Chen, X. Xie, J. Qi, H. Lippold, D. Luo, C. Wang, L. Su, L. He, Q. Wu, Thallium transformation and partitioning during Pb–Zn smelting and environmental implications, Environ. Pollut. 212 (2016) 77–89. DOI: 10.1016/j.envpol.2016.01.046

J. Liu, M. Yin, X. Luo, T. Xiao, Z. Wu, N. Li, J. Wang, W. Zhang, H. Lippold, N.S. Belshaw, Y. Feng, Y. Chen, The mobility of thallium in sediments and source apportionment by lead isotopes, Chemosphere 219 (2019) 864-874. DOI: 10.1016/j.chemosphere.2018.12.041

J. Liu, M. Yin, T. Xiao, C. Zhang, D.C.W. Tsang, Z. Bao, Y. Zhou, Y. Chen, X. Luo, W. Yuan, J. Wang, Thallium isotopic fractionation in industrial process of pyrite smelting and environmental implications, J. Hazard. Mater. 384 (2020) 121378. DOI: 10.1016/j.jhazmat.2019.121378

S.G. Nielsen, M. Rehkämper, A.A.H. Teagle, D.A. Butterfield, J.C. Alt, A.N. Halliday, Hydrothermal fluid fluxes calculated from the isotopic mass balance of thallium in the ocean crust, Earth Planet. Sci. Lett. 251 (2006a) 120–133. DOI: 10.1016/j.epsl.2006.09.002

S.G. Nielsen, M. Rehkämper, M.D. Norman, A.N. Halliday, D. Harrison, Thallium isotopic evidence for ferromanganese sediments in the mantle source of Hawaiian basalts, Nature 439 (2006b) 314–317. DOI: 10.1038/nature04450

S.G. Nielsen, L.E. Wasylenki, M. Rehkämper, C.L. Peacock, Z. Xue, E.M. Moon, Towards an understanding of thallium isotope fractionation during adsorption to manganese oxides, Geochim. Cosmochim. Acta 117 (2013) 252–265. DOI: 10.1016/j.gca.2013.05.004

S.G. Nielsen, M. Rehkämper, J. Prytulak, Investigation and application of thallium isotope fractionation, Rev. Mineral. Geochemistry 82 (2017) 759–798. DOI: 10.2138/rmg.2017.82.18

Z. Ning, E. Liu, D. Yao, T. Xiao, L. Ma, Y Liu, H. Li, C. Liu, Contamination, oral bioaccessibility and human health risk assessment of thallium and other metal(loid)s in farmland soils around a historic Tl-Hg mining area, Sci. Total Environ. 758 (2021) 143577. DOI: 10.1016/j.scitotenv.2020.143577

C.M. Ostrander, S.G. Nielsen, J.D. Owens, B. Kendall, G.W. Gordon, S.J. Romaniello, A.D. Anbar, Fully oxygenated water columns over continental shelves before the Great Oxidation Event, Nature Geoscience 12 (2019) 186–191. DOI: 10.1038/s41561-019-0309-7

C.M. Ostrander, J.D. Owens, S.G. Nielsen, T.W. Lyons, Y. Shu, X. Chen, E.A. Sperling, G. Jiang, D.T. Johnston, S.K Sahoo, A.D. Anbar, Thallium isotope ratios in shales from South China and northwestern Canada suggest widespread O_2 accumulation in marine bottom waters was an uncommon occurrence during the Ediacaran Period, Chem. Geol. 557 (2020) 119856. DOI: 10.1016/j.chemgeo.2020.119856

J.D. Owens, S.G. Nielsen, T.J. Horner, C.M. Ostrander, L.C. Peterson, Thallium-isotopic compositions of euxinic sediments as a proxy for global manganese-oxide burial. Geochim. Cosmochim. Acta 213 (2017) 291–307. DOI: 10.1016/j.gca.2017.06.041

C.L. Peacock, E.M. Moon, Oxidative scavenging of thallium by birnessite: Explanation for thallium enrichment and stable isotope fractionation in marine ferromanganese precipitates, Geochim. Cosmochim. Acta 84 (2012) 297–313. DOI: 10.1016/j.gca.2012.01.036

S.L. Phillips, D.L. Perry, Eds., Handbook of Inorganic Compounds; CRC Press: Boca Raton, FL, 1995.

J. Prytulak, S.G. Nielsen, T. Plank, M. Barker, T. Elliot, Assessing the utility of thallium and thallium isotopes for tracing subduction zone inputs to the Mariana arc, Chem. Geol. 345 (2013) 139–149. DOI: 10.1016/j.chemgeo.2013.03.003

607 J. Prytulak, A. Brett, M. Webb, T. Plank, M. Rehkämper, P.S. Savage, J. Woodhead,
608 Thallium elemental behavior and stable isotope fractionation during magmatic processes,
609 Chem. Geol. 448 (2017) 71–83. DOI: 10.1016/j.chemgeo.2016.11.007
610
611 S.T. Rader, F.K. Mazdab, M.D. Barton, Mineralogical thallium geochemistry and isotope
612 variations from igneous, metamorphic, and metasomatic systems, Geochim. Cosmochim.
613 Acta 243 (2018) 42–65. DOI: 10.1016/j.gca.2018.09.019
614
615 S.T. Rader, R M. Maier, M.D. Barton, F.K. Mazdab, Uptake and fractionation of thallium by
616 *Brassica juncea* in a geogenic thallium-amended substrate, Environ. Sci. Technol. 53 (2019)
617 2441–2449. DOI: 10.1021/acs.est.8b06222
618
619 M. Rehkämper, M. Frank, J. R. Hein, D. Porcelli, A. Halliday, J. Ingri, V. Liebetrau, Thallium
620 isotope variations in seawater and hydrogenetic, diagenetic, and hydrothermal
621 ferromanganese deposits, Earth Planet. Sci. Lett. 197 (2002) 65–81. DOI: 10.1016/S0012-
622 821X(02)00462-4
623
624 M. Rehkämper, M. Frank, J.R. Hein, A. Halliday, Cenozoic marine geochemistry of thallium
625 deduced from isotopic studies of ferromanganese crusts and pelagic sediments, Earth Planet.
626 Sci. Lett. 219 (2004) 77–91. DOI: 10.1016/S0012-821X(03)00703-9
627
628 A. Tremel, P. Masson, T. Sterckeman, D. Baize, M. Mench, Thallium in French agrosystems–
629 I. thallium contents in arable soils, Environ. Pollut. 95 (1997) 293–302. DOI: 10.1016/S0269-
630 7491(96)00145-5
631

A. Vaněk, T. Grygar, V. Chrastný, V. Tejnecký, P. Drahota, M. Komárek. Assessment of the BCR sequential extraction procedure for thallium fractionation using synthetic mineral mixtures, J. Hazard. Mater. 176 (2010) 913–918. DOI: 10.1016/j.jhazmat.2009.11.123

A. Vaněk, M. Komárek, P. Vokurková, M. Mihaljevič, O, Šebek, G. Panušková, V. Chrastný, O. Drábek, Effect of illite and birnessite on thallium retention and bioavailability in contaminated soils, J. Hazard. Mater. 191 (2011) 190–196. DOI: 10.1016/j.jhazmat.2011.04.065

A. Vaněk, M. Mihaljevič, I. Galušková, V. Chrastný, M. Komárek, V. Penížek, T. Zádorová, O. Drábek, Phase-dependent phytoavailability of thallium – A synthetic soil experiment, J. Hazard. Mater. 250-251 (2013) 265–271. DOI: 10.1016/j.jhazmat.2013.01.076

A. Vaněk, Z. Grösslová, M. Mihaljevič, J. Trubač, V. Ettler, L. Teper, J. Cabala, J. Rohovec, T. Zádorová, V. Penížek, L. Pavlů, O. Holubík, K. Němeček, J. Houška, O. Drábek, C. Ash, Isotopic tracing of thallium contamination in soils affected by emissions from coal-fired power plants, Environ. Sci. Technol. 50 (2016) 9864–9871. DOI: 10.1021/acs.est.6b01751

A. Vaněk, Z. Grösslová, M. Mihaljevič, V. Ettler, J. Trubač, V. Chrastný, V. Penížek, L. Teper, J. Cabala, A. Voegelin, T. Zádorová, V. Oborná, O. Drábek, O. Holubík, J. Houška, L. Pavlů, C. Ash, Thallium isotopes in metallurgical wastes/contaminated soils: A novel tool to trace metal source and behavior, J. Hazard. Mater. 343 (2018) 78–85. DOI: 10.1016/j.jhazmat.2017.09.020

A. Vaněk, O. Holubík, V. Oborná, M. Mihaljevič, J. Trubač, V. Ettler, L. Pavlů, P. Vokurková, V. Penížek, T. Zádorová, A. Voegelin, Thallium stable isotope fractionation in white mustard: Implications for metal transfers and incorporation in plants, J. Hazard. Mater. 369 (2019) 521–527. DOI: 10.1016/j.jhazmat.2019.02.060

A. Vaněk, A. Voegelin, M. Mihaljevič, V. Ettler, J. Trubač, P. Drahota, M. Vaňková, V. Oborná, K. Vejvodová, V. Penížek, L. Pavlů, O. Drábek, P. Vokurková, T. Zádorová, O. Holubík, Thallium stable isotope ratios in naturally Tl-rich soils, Geoderma 364 (2020) 114183. DOI: 10.1016/j.geoderma.2020.114183

K. Vejvodová, A. Vaněk, M. Mihaljevič, V. Ettler, J. Trubač, M. Vaňková, P. Drahota, P. Vokurková, V. Penížek, T. Zádorová, V. Tejnecký, L. Pavlů, O. Drábek, Thallium isotopic fractionation in soil: the key controls, Environ. Pollut. 265 (2020) 114822. DOI: 10.1016/j.envpol.2020.114822

A. Voegelin, N. Pfenninger, J. Petrikis, J. Majzlan, M. Plötze, A.C. Senn, S. Mangold, R. Steininger, J. Göttlicher, Thallium speciation and extractability in a thallium- and arsenic-rich soil developed from mineralized carbonate rock, Environ. Sci. Technol. 49 (2015) 5390–5398. DOI: 10.1021/acs.est.5b00629

X. Wei, J. Wang, J. She, J. Sun, J. Liu, Y. Wang, X. Yang, Q. Ouyang, Y. Lin, T. Xiao, D.C.W. Tsang, Thallium geochemical fractionation and migration in Tl-As rich soils: The key controls, Sci. Total Environ. 784 (2021) 146995. DOI: 10.1016/j.scitotenv.2021.146995

J. Wiederhold, Metal stable isotope signatures as tracers in environmental geochemistry, Environ. Sci. Technol. 49 (2015) 2606−2624. DOI: 10.1021/es504683e

T. Xiao, J. Guha, D. Boyle, C.Q. Liu, J. Chen, Environmental concerns related to high thallium levels in soils and thallium uptake by plants in southwest Guizhou, China, Sci. Total Environ. 318 (2004) 223–244. DOI: 10.1016/s0048-9697(03)00448-0

T. Xiao, F. Yang, S. Li, B. Zheng, Z. Ning, Thallium pollution in China: A geo-environmental perspective, Sci. Total Environ. 421–422 (2012) 51–58. DOI: 10.1016/j.scitotenv.2011.04.008

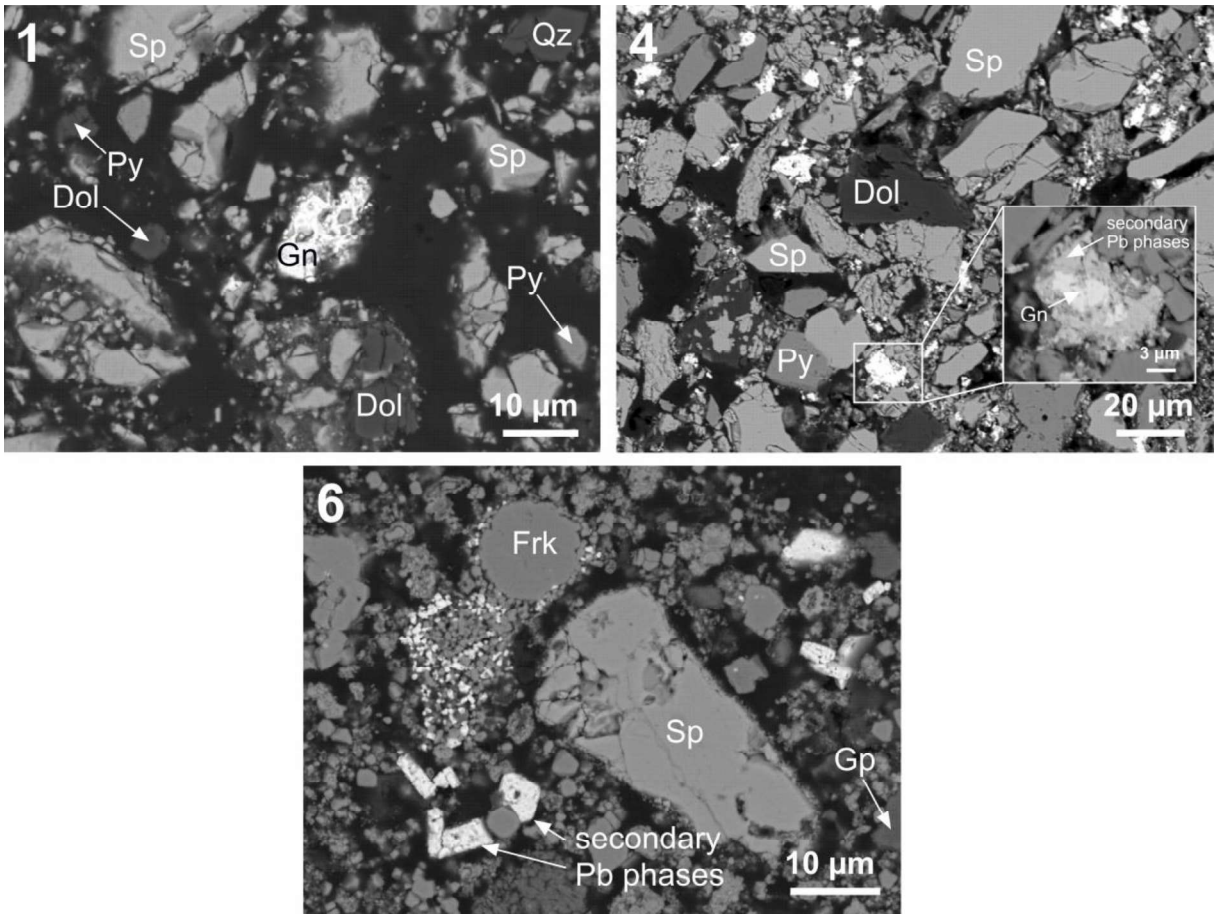

Figure 1. Scanning electron micrographs in back-scattered electrons (SEM-BSE) of selected sulfide concentrates (no. 1 and 4) and a metallurgical waste/sludge (no. 6). Fragments of sphalerite, pyrite and galena associated with the gangue dolomite and quartz (1 – Lisheen, Ireland); fragments of sphalerite, pyrite and gangue dolomite with residues of galena grains altered to a mixture of secondary Pb phases (4 – Olkusz, Poland); fragments of sphalerite, franklinite and gypsum associated with a mixture of Pb-rich secondary weathering products (6 – Larox sludge). Phase abbreviations: Dol – dolomite ($CaMg(CO_3)_2$); Frk – franklinite ($ZnFe_2O_4$); Gn – galena (PbS); Gp – gypsum ($CaSO_4 \cdot 2H_2O$); Py – pyrite (FeS_2); Sp – sphalerite (ZnS); Qz – quartz (SiO_2).

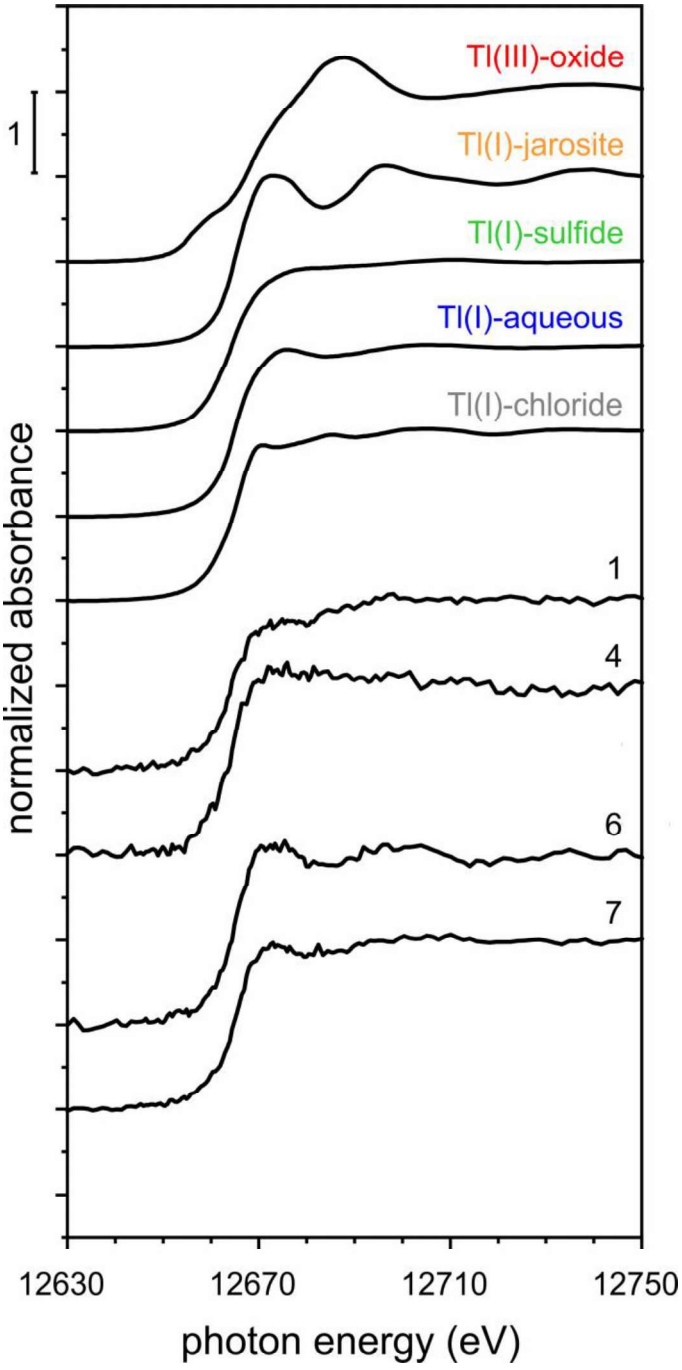

Figure 2. Normalized Tl L_{III}-edge XANES spectra in selected sulfide concentrates (no. 1 and 4) and metallurgical wastes/sludges (no. 6 and 7), compared with reference spectra for Tl(III)-oxide (Tl_2O_3, avicenite), Tl-jarosite, Tl-sulfide ($TlAsS_2$, lorandite), aqueous Tl^+ and Tl(I)-chloride. 1 – Lisheen, Ireland; 4 – Olkusz, Poland; 6 and 7 – Larox and Dorr sludges. Detailed information about the samples is available in the Supplementary Material section.

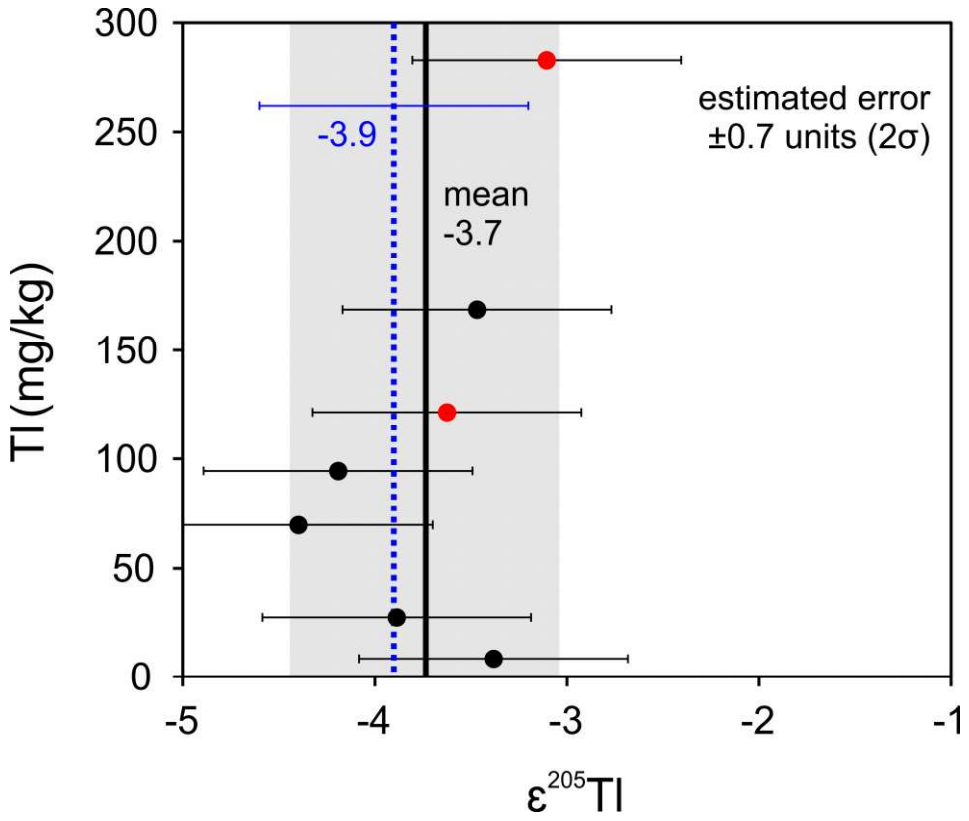

Figure 3. Thallium concentration in the studied sulfide concentrates, the post-flotation waste and the metallurgical wastes/sludges (red points) vs. ε^{205}Tl. Black bold line depicts an unweighted mean ε^{205}Tl value calculated from all the samples (-3.7), blue dotted line depicts a calculated model ε^{205}Tl value for the metallurgical feed (-3.9). An estimated error of ±0.7 ε^{205}Tl (2σ) is based on our external reproducibility of multiple separate analyses of the SRM AGV-2 (USGS, USA) (Table S3, Supplementary Material).

Table 1. Thallium/element concentrations and Tl isotopic signatures (ε^{205}Tl) in the studied Zn-rich sulfide concentrates, the post-flotation waste and the metallurgical waste samples (Larox and Dorr sludges). Detailed information about the samples is available in the Supplementary Material section.

No.	Description	Tl	Zn	Pb	Fe	ε^{205}Tl ± 0.7
		mg/kg	g/kg	g/kg	g/kg	
1	Lisheen, Ireland – concentrate (ZnS)	169±4	500±38	25±2	47±6	-3.47
2	Pinargozu, Turkey – concentrate (ZnS)	8.64±0.24	499±34	47±2	44±6	-3.39
3	Olkusz, Poland – concentrate (ZnS)	70.1±12.8	554±156	18±2	30±10	-4.40
4	Olkusz, Poland – concentrate/reflot (ZnS+PbS)	94.8±3.6	366±30	147±20	71±6	-4.20
5	Olkusz, Poland – post-flotation waste (ZnS)	27.6±3.0	116±42	25±5	---	-3.89
6	Larox sludge (50% Olkusz and 50% mix Lisheen/Pinargozu)	122±0	180±88	123±2	194±98	-3.63
7	Dorr sludge (50% Olkusz and 50% mix Lisheen/Pinargozu)	283±34	245±102	79±2	135±56	-3.11
	A smelter feed material (charge)*	~86	---	---	---	~-3.9

The Tl/metal concentrations are reported at the 2σ level (n = 3).
The ε^{205}Tl results assign an estimated error of ±0.7 ε^{205}Tl (2σ) which is based on our external reproducibility of multiple separate analyses of the SRM AGV-2 (USGS, USA) (Table S3). "Reflot" means a metal-rich concentrate prepared by recycling of mine waste, i.e., by flotation. *Data obtained by a weighted mean calculation from the Olkusz, Lisheen and Pinargozu concentrate data in a mixing ratio of ~2/~1/~1, respectively; see the Supplementary Material section for details. ---: not determined.

SUPPLEMENTARY MATERIAL

Evaluation of thallium isotopic fractionation during the metallurgical processing of sulfides: an update

Aleš Vaněk[a,*], Kateřina Vejvodová[a], Martin Mihaljevič[b], Vojtěch Ettler[b], Jakub Trubač[b], Maria Vaňková[b], Leslaw Teper[c], Jerzy Cabala[c], Katarzyna Sutkowska[c], Andreas Voegelin[d], Jörg Göttlicher[e], Ondřej Holubík[a], Petra Vokurková[a], Lenka Pavlů[a], Ivana Galušková[a], Tereza Zádorová[a]

[a] Department of Soil Science and Soil Protection, Faculty of Agrobiology, Food and Natural Resources, Czech University of Life Sciences Prague, Kamýcká 129, 165 00 Praha 6, Czech Republic

[b] Institute of Geochemistry, Mineralogy and Mineral Resources, Faculty of Science, Charles University, Albertov 6, 128 00 Praha 2, Czech Republic

[c] Institute of Earth Sciences, Faculty of Natural Sciences, University of Silesia, Bedzinska 60, 41-200 Sosnowiec, Poland

[d] Eawag, Swiss Federal Institute of Aquatic Science and Technology, Ueberlandstrasse 133, CH-8600 Duebendorf, Switzerland

[e] Institute for Photon Science and Synchrotron Radiation, Karlsruhe Institute of Technology, KIT Campus North, Hermann-von-Helmholtz-Platz 1, D-76344 Eggenstein-Leopoldshafen, Germany

5 CHAPTERS, 2 FIGURES, 7 TABLES (12 PAGES)

I. SAMPLE DESCRIPTION

Sample 1.

Concentrate from ores of the Lisheen Zn-Pb-Ag deposit
Localization: County Tipperary in southeast-central Ireland

Description of the deposit: Mississippi Valley type. Hydrothermal origin. Strata-bound pyritic sulfide lenses containing 22 Mt of ore with an overall grade of 11.5 percent Zn, 1.9 percent Pb, 26 g/t Ag, and 16 percent Fe. Ores are hosted in Lower Carboniferous (Early Mississippian) carbonate rocks. Sulfide bodies consist of pyrite-marcasite, sphalerite, and galena with subsidiary sulfosalt minerals, arsenopyrite, and copper sulfides. Sulfides replace carbonate minerals and infill dissolution cavities. Gangue minerals intergrown with sulfides include dolomite, calcite, barite, and quartz (Hitzman et al., 2002).

Sample 2.

Concentrate from ores of the Pinargozu deposit
Localization: Province of Adana, south-central Turkey

Description of the deposit: Mississippi Valley type. Hydrothermal origin. Formed within the passive-margin platform carbonate sequences with fluid-flow system related to the Cimmerian or Alpine orogenic compression. Mining has mainly been of secondary zinc mineralization, formed due to supergene oxidation of massive sulfides. Primary mineralization is dominant in deeper parts, where coarse massive-sphalerite-rich sulfide with pyrite, massive galena occur. Secondary mineralization is represented by smithsonite, hemimorphite and smaller amount of hydrozincite, and is associated with abundant Fe-oxidee and hydrooxides and cerussite. Zn and Pb are accompanied by general tenor of >50 g/t silver, locally >250 g/t (https://miningdataonline.com).

Sample 3.

ZnS concentrate from ores of Olkusz deposit
Localization: Southern Poland

Description of the deposit: The Zn–Pb ore mineralization is of low temperature hydrothermal Mississippi Valley-Type. The age of metals emplacement is assumed to be between 150-200Ma (Jacher-Śliwczyńska, 2008) and 138.5 Ma (Sutkowska, 2009). The host rocks to the ore bodies are Middle Triassic limestones altered to ore-bearing dolomites. The bulk of the mineralization comprises strata-bound galena and/or sphalerite with associated pyrite and marcasite. Typical associated elements are Cd, Ag, Tl, As, Ba and Mn (Cabala and Teper, 2007).

Sample 4.

Reflot ZnS+PbS concentrate from ores of Olkusz deposit
Localization: Southern Poland

This is the concentrate produced by flotation of post-flotation wastes deposited in tailings pond located at Olkusz. The wastes come solely from the Olkusz ores processing (for the characterization, see sample 3 description)

Sample 5.

Post-flotation waste from ores of Olkusz deposit
Localization: Southern Poland

This is a waste material produced by flotation of the Olkusz ores (for the characterization, see sample 3 description).

Samples 6. and 7.

Larox and Dorr sludges

Localization: Boleslaw, Southern Poland

Description of the material: Material consisting of the Olkusz (50%) and mixed Lisheen/Pinargozu (50%) concentrates is used in the Boleslaw processing plant (near Olkusz). The leaching process is adopted to treat only the calcine of the zinc oxides produced from the Waelz fumes by calcination in a rotary kiln. Slurry obtained is prepared for further processing by solution purification and zinc electrolysis. The slurry is classified in hydrocyclones. The overflow from the hydrocyclones is transported by gravity to Dorr thickeners. The overflow from the thickeners is pumped to a solution purification plant and the underflow (the pulp which constitutes sample 7) is pumped to low acid leaching tanks. After classification, the pulp is washed and filtered at Larox filters. The cake from the filters (sample 6) is transported by conveyors to the pyrometallurgical plant (Fig. S1).

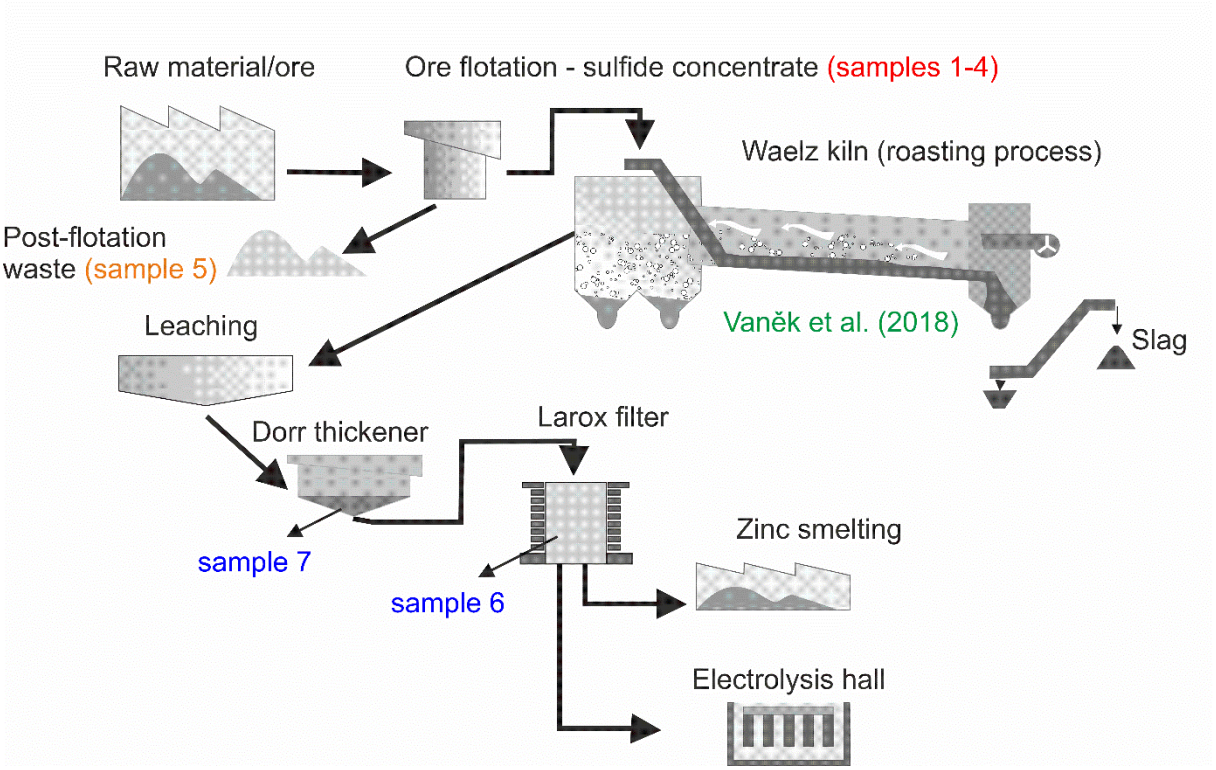

Figure S1. Simplified Zn metallurgical processing flowsheet showing ore concentrate (1-4), post-flotation waste sample (5) and metallurgical waste sample (sludge) locations (6 and 7).

II. MINERALOGICAL INVESTIGATIONS

Table S1. Operating conditions of the EPMA, standards and detection limits for the measurements of sulfides and oxides, respectively.

Sulfides

accelerating voltage 20 kV, beam current 30 nA, focused beam size

Element	X-ray	Crystal	Standard	Detection limit (wt.%) - elements
As	La	TAP	Gallium Arsenide	0.018
S	Ka	PETJ	Marcasite	0.004
Pb	Ma	PETJ	Galena	0.019
Zn	Ka	LIF	Sphalerite	0.012
Fe	Ka	LIFL	Marcasite	0.007
Tl	La	LIFL	Thallium Bromide/iodide	0.020

Oxides

accelerating voltage 15 kV, beam current 30 nA, focused beam size

Element	X-ray	Crystal	Standard	Detection limit (wt.%) - oxides
Si	Ka	TAP	Quartz	0.03
Al	Ka	TAP	Al_2O_3	0.02
K	Ka	PETJ	Sanidine	0.02
Ca	Ka	PETJ	Diopside	0.02
S	Ka	PETJ	Anhydrite	0.13
Pb	Ma	PETJ	Crocoite	0.04
Cd	La	PETJ	Cadmium Metal	0.02
Fe	Ka	LIFL	Magnetite	0.03
Mn	Ka	LIFL	Rhodonite	0.03
Zn	Ka	LIFL	Willemite	0.05
Tl	La	LIFL	Thallium Bromide/Iodide	0.11
Na	Ka	TAP	Albite	0.02
Mg	Ka	TAP	MgO	0.01

III. QUALITY CONTROL OF THALLIUM DETERMINATION

Table S2. Measured and certified Tl values for standard reference material, NIST 2711 (Montana Soil) (National Institute of Standards and Technology, USA) The analysis was carried out in triplicate and depict mean (2σ).

	Measured (mg/kg)	Certified (mg/kg)
NIST 2711	2.31 ± 0.39	2.47 ± 0.30

IV. STABLE THALLIUM ISOTOPE SEPARATION AND MEASUREMENT

In order to isolate Tl from the sample matrix (i.e., digested sample), a two-stage chromatographic separation with an anion exchange resin (Bio-Rad AG1-X8, 200-400 mesh, Cl^- cycle) was performed. The sample was evaporated to complete dryness and then redissolved in 0.1 M HCl. Subsequently, Br_2 was added so that the reagent had a final concentration of 1% (v/v) in the sample solution (0.1 M HCl). The solution was then left overnight (>12 h) to ensure that all the Tl(I) was oxidized to Tl(III). For Tl separation, a sample aliquot was taken so that, in general, 100-500 ng of total Tl was present. The first stage of the chromatography utilized a 10-mL Poly-Prep-column (Bio-Rad, USA) filled with 2 mL of resin, followed by steps with reagent mixtures and volumes as follows: (i) 5×1 mL 0.1 M HCl-SO_2 + 5×1 mL 0.1 M HCl, resin cleaning; (ii) 5×2 mL 0.1 M HCl-1% Br_2, resin treatment; (iii) sample loading (0.1 M HCl-1% Br_2); (iv) 10×2 mL 0.01 M HCl-1% Br_2; (v) 6×2 mL 0.5 M HNO_3-1% Br_2; (vi) 6×2 mL 2 M HNO_3-1% Br_2; (vii) 6×2 mL 0.1 M HCl-1% Br_2; (viii) 15×2 mL 0.1 M HCl-SO_2, Tl/Pb fraction elution. The obtained Tl/Pb fraction was evaporated and redissolved in 200 µL 0.1 M HCl-1% Br_2 (>12 h), in preparation for the next part of the Tl purification. A PP 1.2-mL micro-column filled with 250 µL of resin was used for the second chromatographic stage. Resin cleaning and treatment, as well as sample loading, were performed in the same way, with corresponding lower volumes of the individual reagent mixtures. Once the final Tl fraction was obtained, the Tl sample was evaporated and diluted in 5 mL 2% HNO_3. The Tl and Pb concentrations were monitored after sample dissolution and Tl separation. Chemicals of ultrapure and suprapure quality (Merck, Germany) and deionized water (MilliQ+, Millipore, USA) were used for the separation techniques.

Multi-collector inductively coupled plasma mass spectrometry (MC-ICP-MS) (Neptune Plus, Thermo Scientific, Germany) with a desolvating nebulizer (Aridus II, CETAC, USA) was used to determine the Tl isotope ratios. All the solutions were measured in 3 runs (50 cycles each). External normalization (with Pb) and standard sample bracketing (NIST SRM 997) were employed to eliminate the mass bias drift. The $^{208}Pb/^{206}Pb$ ratio was used for the correction of the raw $^{205}Tl/^{203}Tl$ ratio, i.e., using NIST SRM 981 (Common lead) added to the sample to obtain Pb/Tl 2–3. The Tl isotopic composition was calculated using the following equation with ε notation relative to NIST SRM 997 (Eq. 1).

$$\varepsilon^{205}Tl = \frac{^{205}Tl/^{203}Tl_{sample} - ^{205}Tl/^{203}Tl_{NIST\,997}}{^{205}Tl/^{203}Tl_{NIST\,997}} \times 10^4$$

Repeated analyses of the Sigma-Aldrich standard solution (for ICP analysis) resulted in a mean $\varepsilon^{205}Tl$ of –0.80 and –0.90 (n = 3). The estimated error ±0.7 $\varepsilon^{205}Tl$ (2σ) (Table S3) for the

presented sample set is based on our long-term external reproducibility for the standard reference material AGV-2 (Andesite, USGS, USA). This approach encompasses all the critical steps of the complete analytical procedure (sample dissolution, ion exchange chromatography and mass spectrometry).

Table S3. Measured and reference Tl concentration and Tl isotopic data for the standard reference material AGV-2 in our laboratory and by Prytulak et al. for comparison.

Tl (μg/kg)	2σ	ε^{205}Tl	2σ	n	Diss.	References
272	24	**–3.1***	**0.4***	2	1	(Vejvodová et al., 2020)
250	38	**–2.6**	**0.8**	3	3	(Vaněk et al., 2020)
239	30	**–3.2**	**0.6**	2	2	(Vaněk et al., 2018)
282	35	**–2.8***	**0.7***	2	1	(Grösslová et al., 2018)
245	32	**–3.4**	**0.7**	6	6	(Vaněk et al., 2016)
267	35	–3.0	0.6	15	8	(Prytulak et al., 2013)
267	0	–2.7	0.2	9	5	(Prytulak et al., 2017)

*Data calculated from repeated measurements of the same sample.

V. MINERALOGIAL AND THALLIUM SPECIATION DATA

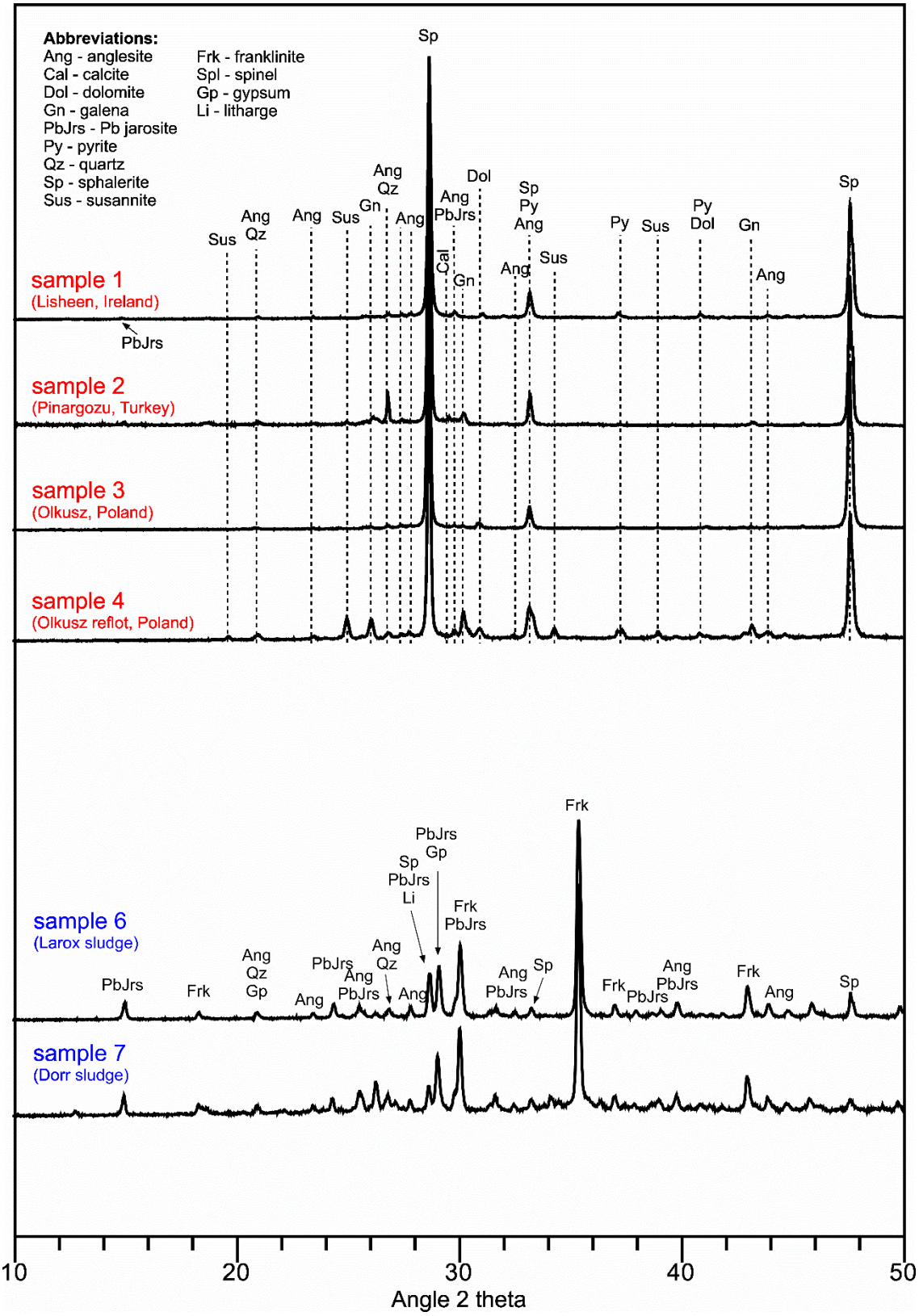

Figure S2. XRD patterns of ore concentrates (1-4) and metallurgical waste samples (6 and 7).

Table S4. Representative microprobe analyses of sulfides in wt.%, at.% and recalculated to structural formulae (*apfu* – atoms per formula unit) on the basis of 1 S+As (sphalerite, galena) and 2 S+As (pyrite).

Phase	sphalerite	sphalerite	sphalerite	pyrite	pyrite	galena
Sample no.	1	4	6	1	4	4
Spot	26	8	19	29	12	10
wt.%						
Fe	0.43	0.91	1.99	48.78	48.30	0.47
Zn	66.68	66.67	65.18	1.73	1.78	4.67
Pb	0.09	0.09	0.09	0.29	0.83	82.77
Tl	**0.09**	**0.06**	**0.03**	**0.07**	**0.04**	**0.20**
As	-	-	-	0.18	-	-
S	32.06	31.77	32.13	51.19	51.42	10.99
Total	99.34	99.49	99.42	102.23	102.37	99.10
at.%						
Fe	0.38	0.80	1.75	34.92	34.59	0.48
Zn	50.28	50.29	48.98	1.06	1.09	4.71
Pb	0.02	0.02	0.02	0.06	0.16	83.52
Tl	**0.02**	**0.01**	**0.01**	**0.01**	**0.01**	**0.20**
As	-	-	-	0.10	-	-
S	49.30	48.88	49.24	63.85	64.15	11.09
apfu						
Fe	0.0077	0.0164	0.0355	1.0923	1.0786	0.0429
Zn	1.0200	1.0289	0.9948	0.0331	0.0340	0.4248
Pb	0.0004	0.0004	0.0004	0.0018	0.0050	7.5303
Tl	**0.0004**	**0.0003**	**0.0001**	**0.0004**	**0.0002**	**0.0179**
As	-	-	-	0.0030	-	-
S	1.0000	1.0000	1.0000	1.9970	2.0000	1.0000

- not detected

Table S5. Representative microprobe analyses of complex mixtures of secondary Pb-bearing phases (anglesite, plumbojarosite, susannite and/or lithagite).

Sample no.	1	4	6	6	6
Spot	6	11	22	24	25
wt.%					
Fe	0.29	2.19	1.84	2.44	2.07
Zn	5.62	23.20	2.11	2.19	1.84
Pb	54.13	19.12	63.29	60.88	58.12
Tl	**0.19**	**0.10**	**0.20**	**0.06**	**0.10**
S	6.58	13.49	7.27	7.25	6.86
Total	66.81	58.10	74.71	72.82	68.99

Table S6. Representative microprobe analyses of spinel-family oxides and a gypsum-like phase.

Phase	spinel	spinel	spinel	gypsum
Sample no.	6	6	6	6
Spot	1	3	7	5
wt.%				
SiO_2	0.04	-	0.35	0.07
Al_2O_3	0.05	0.82	0.12	-
FeO	64.29	60.82	66.80	1.86
MnO	0.05	0.22	2.80	-
MgO	0.11	0.47	0.26	-
CaO	-	0.05	0.25	36.71
Na_2O	0.55	0.59	0.52	-
K_2O	0.14	0.07	-	0.03
PbO	0.06	0.29	0.39	5.04
ZnO	31.66	33.96	26.05	1.36
CdO	1.35	0.64	0.11	0.23
Tl_2O_3 / (Tl)	**0.13 (0.12)**	**0.27 (0.24)**	**0.31 (0.28)**	**0.34 (0.30)**
SO_3	-	-	-	35.07
Total	98.44	98.19	97.96	80.71
*% end members**				
$FeAl_2O_4$ (hercynite)	0.00	1.19	0.03	
$MnAl_2O_4$ (galaxite)	0.00	0.00	0.03	
$ZnAl_2O_4$ (gahnite)	0.11	0.59	0.21	
$MgFe_2O_4$ (magnesioferrite)	0.68	0.90	1.59	
$FeFe_2O_4$ (magnetite)	0.86	65.03	10.45	
$MnFe_2O_4$ (jacobsite)	0.18	0.24	9.61	
$ZnFe_2O_4$ (franklinite)	98.17	32.05	78.08	

- not detected

* % of end members calculated by the EMG software (Ferracutti et al., 2015)

Table S7. Thallium, Pb and Zn concentrations in the operationally-defined chemical fractions obtained within the BCR sequential extraction method (n = 3; RSD ≤10%). The oxidizable and residual element fractions were calculated using the data from total sample digestions.

Sample no. *Fraction*	*concentrate	Tl mg/kg	Pb g/kg	Zn g/kg
Acid-extractable				
1. Lisheen, Ireland	*	10	0	31
2. Pinargozu, Turkey	*	1	0	19
3. Olkusz, Poland	*	4	0	20
4. Olkusz, Poland	*	11	0	25
6. Larox sludge		15	0	10
7. Dorr sludge		19	0	90
Reducible				
1. Lisheen, Ireland	*	8	7	5
2. Pinargozu, Turkey	*	1	8	2
3. Olkusz, Poland	*	2	8	4
4. Olkusz, Poland	*	6	24	3
6. Larox sludge		95	14	10
7. Dorr sludge		264	16	22
Oxidizable + Residual				
1. Lisheen, Ireland	*	151	18	464
2. Pinargozu, Turkey	*	7	39	478
3. Olkusz, Poland	*	64	10	530
4. Olkusz, Poland	*	78	123	338
6. Larox sludge		12	109	160
7. Dorr sludge		0	63	133

REFERENCES

Cabala J.; Teper L. Metalliferous constituents of rhizosphere soils contaminated by Zn-Pb mining in southern Poland. Water, Air, and Soil Pollution 2007, 178, 351-362.

Ferracutti, G.R.; Gargiulo, M.F.; Ganuza, M.L.; Bjerg, E.A.; Castro, S.M. Determination of the spinel group end-members based on electron microprobe analyses. Mineralogy and Petrology 2015, 109, 153-160.

Grösslová, Z.; Vaněk, A.; Oborná, V.; Mihaljevič, M.; Ettler, V.; Trubač, J.; Drahota, P.; Penížek, V.; Pavlů, L.; Sracek, O.; Kříbek, B.; Voegelin, A.; Göttlicher, J.; Ondřej, D.; Tejnecký, V.; Houška, J.; Mapani, B.; Zádorová, T. Thallium contamination of desert soil in Namibia: chemical, mineralogical and isotopic insights. Environmental Pollution 2018, 239, 272-280.

Hitzman M.W.; Redmond P.B.; Beaty D. W. The carbonate-hosted Lisheen Zn-Pb-Ag deposit, County Tipperary, Ireland. Economic Geology 2002, 97, 1627-1655.

Jacher-Śliwczyńska K., 2008. Source of lead and origin of Silesian-Cracow Zn-Pb ore deposits based on isotopic study. PhD Thesis, Jagiellonian University Krakow (in Polish).

Prytulak, J.; Nielsen, S. G.; Plank, T.; Barker, M.; Elliot, T. Assessing the utility of thallium and thallium isotopes for tracing subduction zone inputs to the Mariana arc. Chemical Geology 2013, 345, 139-149.

Prytulak, J.; Brett, A.; Webb, M.; Plank, T.; Rehkämper, M.; Savage, P. S.; Woodhead, J. Thallium elemental behavior and stable isotope fractionation during magmatic processes. Chemical Geology 2017, 448, 71-83.

Sutkowska K., 2009. Tectonic structures and metallogeny of Chrzanów Zn-Pb ore district. PhD Thesis, University of Silesia, Katowice (in Polish).

Vaněk, A.; Voegelin, A.; Mihaljevič, M.; Ettler, V.; Trubač, J.; Drahota, P.; Vaňková, M.; Oborná, V.; Vejvodová, K.; Penížek, V.; Pavlů, L.; Drábek, O.; Vokurková, P.; Zádorová, T.; Holubík, O. Thallium stable isotope ratios in naturally Tl-rich soils. Geoderma 2020, 364, 114183.

Vaněk, A.; Grösslová, Z.; Mihaljevič, M.; Ettler, V.; Trubač, J.; Chrastný, V.; Penížek, V.; Teper, L.; Cabala, J.; Voegelin, A.; Zádorová, T.; Oborná, V.; Drábek, O.; Holubík, O.; Houška, J.; Pavlů, L.; Ash, C. Thallium isotopes in metallurgical wastes/contaminated soils: A novel tool to trace metal source and behavior. Journal of Hazardous Materials 2018, 343, 78-85.

Vaněk, A.; Grösslová, Z.; Mihaljevič, M.; Trubač, J.; Ettler, V.; Teper, L.; Cabala, J.; Rohovec, J.; Zádorová, T.; Penížek, V.; Pavlů, L.; Holubík, O.; Němeček, K.; Houška, J.; Drábek, O.; Ash, C. Isotopic tracing of thallium contamination in soils affected by emissions from coal-fired power plants. Environmental Science and Technology 2016, 50 (18), 9864-9871.

Vejvodová, K.; Vaněk, A.; Mihaljevič, M.; Ettler, V.; Trubač, J.; Vaňková, M.; Drahota, P.; Vokurková, P.; Penížek, V.; Zádorová, T.; Tejnecký, V.; Pavlů, L.; Drábek, O. Thallium isotopic fractionation in soil: the key controls. Environmental Pollution 2020, 265, 114822.

https://miningdataonline.com/property/3221/Pinargozu-Mine.aspx#Geology